PROCEEDINGS, Twenty-Seventh Workshop on Geothermal Reservoir Engineering
Stanford University, Stanford, California, January 28-30, 2002
SGP-TR-171

LARGE-SCALE MICROSIESMIC/ERT LABORATORY EXPERIMENTS TO DETERMINE EGS RESPONSE TO WATER INJECTION

Steven D. Glaser, Jeffrey Moore, Hee-Joon Kim[1], Mark Talesnick[2]

University of California
440 Davis Hall
Berkeley, CA 94720, USA
e-mail: glaser@ce.berkeley.edu

ABSTRACT

We present a large-scale testing system for determining the precise physical mechanisms at work when ambient temperature water is injected into a high temperature geothermal reservoir. The poly-axial testing chamber can apply up to 14 MPa loads on 3 independent axes using flat-jacks as the loading mechanism. The chamber can be flooded by up to 300° C steam, so that the rock can be brought to in situ equilibrium. Heat can also be applied by four 2 kW heaters around the block perimeter, with the additional application of modeling hot dry rock systems. Steam at an appropriate quality is used as the pore fluid so that field electro-resistive behavior and in situ effective stresses can be accurately modeled. To account for the actual fractured nature of the in situ rock mass, size effects of fracture toughness, and to undo averaging of electro-resistive properties, the specimens will be 260 mm cubic assemblages made up of outcrop rock representative of reservoir rock. Fracturing of the sample will be monitored by a dense array of resistivity sensors, which will be used to create a real-time tomograph. The paper describes the full system and gives examples of the suitability of using electro-resistive tomography for forward and inverse imaging.

PROJECT PURPOSE

The Geysers Geothermal field in northern California is currently undergoing enhanced thermal recovery by injection of local wastewater. This process is illustrated by the cartoon shown in Figure 1. We want to determine what physical mechanisms are at work when ambient temperature water is injected into a high temperature geothermal reservoir, and the attainment of certainty as to which mechanisms control behavior. We want to image the actual damage mechanics at work, the geo-hydrology at work, and how these (or other) mechanisms affect field measurements. We make use of laboratory resistivity measurements and permeability estimates of matrix rock at reservoir conditions to aid interpretation of our electro-resistive tomography (ERT) measurements. Scaling issues associated with the time evolution of resistivity anomalies with experiments and flow modeling will be addressed. This fundamental understanding of the injection-resistivity process will allow quantitative interpretation of the upcoming cross-well electromagnetic imaging to be conducted by Electromagnetic Instruments Inc. under DOE funding.

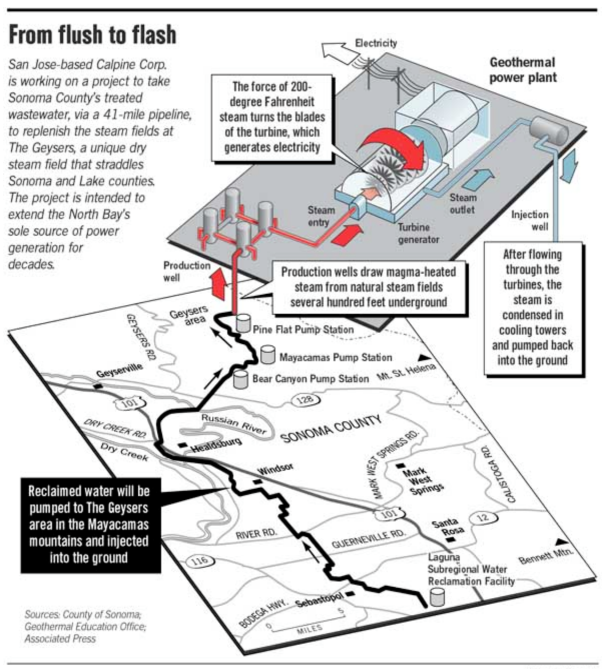

Figure 1 Recharge of The Geysers geothermal field by wastewater injection (San Francisco Chronicle, 10 July, 2001.

Project Objective(s)

• Providing a basis for improved interpretation of microseismic and electrical data to identify, image,

[1] Pukyong University, Pusan, Korea; [2] The Technion, Haifa, Israel

and characterize fluid flow paths in geothermal reservoirs;

• Demonstration of how routine measurement of physical properties, combined with acoustic and electromagnetic emission data interpretation, can be used to improve conventional geothermal reservoir simulation; and finally

• Providing a quantitative and objective approach for managing the increasing injection rates in a geothermal field, including enhanced recovery techniques.

The project combines microseismic imaging of damage kinematics and electro-resistive tomography laboratory experiments with in situ data to define the reaction of enhances geothermal systems to water injection. From these predictions, a set of guidelines will be developed to optimize the production/injection strategy.

Plans and Approach

Our experiment isolates the physical processes of interest in as realistic an environment as possible. To account for the actual fractured nature of the in situ rock mass, size effects of fracture toughness, and undo averaging of electro-resistive properties, the specimens will be 260 mm cubic assemblages made up of outcrop graywacke representative of reservoir conditions. The polyaxial testing chamber can apply up to 14 MPa loads on 3 independent axes using flat-jacks as the loading mechanism. The chamber can be flooded by up to 300° C steam, so that the rock can be brought to in situ equilibrium. Heat can also be applied by four 2 kw heaters around the block perimeter. Steam with an appropriate quality is used as the pore fluid so that field electroresistive behavior and in situ effective stresses can be accurately modeled.

Passive acoustic monitoring during injection of water through a small wellbore will localize and characterize dislocation sources from natural and induced crack interfaces, using an approach based on fundamental physical principles. The challenge is to develop a methodology to interpret those signals, first in the laboratory under controlled and known conditions, and then to migrate this understanding to the field. Given the fine microseismic surveys made by previous DOE contractors at a variety of thermal fields such as the Geysers (e.g. Stark, 1990), operators will be able to better utilize microseismic data after we provide correlations with known mechanics.

Our approach involves the location of events, and characterization of source kinematics through a second-order time domain moment tensor calculated from full waveforms rather than first P-wave arrivals (e.g. Stump and Johnson, 1969). This method completely describes the equivalent force-time histories that make up an event, from analysis of the eigenvalues and eigenvectors. The resulting vectors form a parametric model that captures time and frequency characteristics of the original data, and identifies critical features extracted from each sensor signal.

A major objective of the resistivity experiment will be to energize current-voltage configurations that will facilitate measurement of resistivity anisotropies induced by fracture and stress anisotropies. The system will directly measure the resistivities associated with the changing water-steam phases in the sample and the anisotropy brought about by preferential flows/fluid content in the fractures. The same low-noise electrode arrays will also measure the voltages generated by fluid or steam flow.

Arrays of electrodes are installed on the rock faces to simultaneously monitor the resistivity changes and streaming potentials. Small contact area non-polarizing electrodes have been developed for injecting current and measuring voltages on the surface of rock or concrete.

Testing Device

The insides of the testing device, shown in Fig. 2, contains a cubical sample with a centered borehole extending to a depth of half the sample height. The polyaxial in situ stress is modeled by the stresses applied via hydraulic pressure in 20-gauge steel flat jacks.

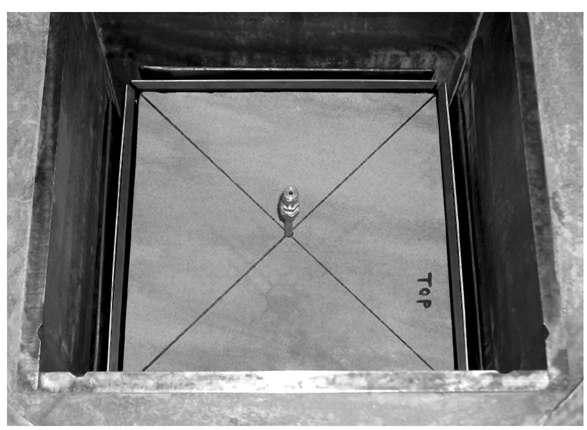

Figure 2 The inside of the high-pressure test chamber, showing the 260 mm cubic specimen with a 9 mm diameter injection well-point. From the specimen out are layers of PEEK, aluminum with integral heaters, flat jack, and cell wall.

Once the in situ thermal and stress equilibrium is attained, cool water is injected into the borehole through the top of the testing device. The amount of water injected will be either a constant volume, or at a constant rate, depending on the application. Fracturing of the sample will be monitored by a dense array of resistivity sensors, which will be used to create a real-time tomograph. The hydraulic force is generated by three independently controlled air/hydraulic intensifiers which can be seen at the right side of Fig. 3.

The sample is surrounded by plate assemblies which have a dense machined grid to allow for unimpeded movement of steam and condensate around the sample. On the back of each plate is a machined groove holding a 2000W coil heater, which can be used simultaneously with the steam, or independently, as in modeling a hot-dry-rock system. A 6 mm grooved PEEK plate is the contact layer with the specimen (so that current flows through the rock rather than short-circuiting through the device).

Steam (126 lb/hr) is produced in a Lattner 480V, 2 MPa electric boiler fed by pre-heated water. Furthermore, the sample will be preheated using the 2000W coil heaters previously described (preheating may also be necessary to deactivate the clays in the sample, as in field conditions).

The system is overseen by computer controlled servo loops. In addition to the ERT and microseismic measurements, Table 1 lists process variables that are being continuously monitored, controlled, and recorded.

Figure 3 Overview of the testing device. From the left of the picture: boiler, pressure cell with insulation jacket, pressure intensifiers, computer control station (Talesnick in command).

Table 1 Process variables monitored, controlled, and recorded during a test.

Boiler energy consumption	Inlet steam pressure
3-D "in situ" stress	Hydraulic oil temperature
Water volume into system	Water volume out of system
Injection volume	Injection temperature
Injection pressure	Inlet steam temperature
Rock internal temperature	Superheat energy

ELECTROMAGNETIC IMAGING

The advancing injection fluid front will change in situ resistivity which can be mapped, possibly from the surface, but certainly using new techniques of cross hole and surface to bore hole electrical resistivity tomography (ERT) or electromagnetic (EM) imaging. Streaming potentials associated with these kinematics will provide an independent measure of the locations of principal flow paths.

None of the geophysical techniques suggested here are themselves new. There have been many studies in which acoustic emissions have been used to identify dynamic portions of a geothermal reservoir during normal production, but without absolute physical calibration of the actual mechanisms and without ERT. Resistivity and EM methods have been used to define high temperature regions and to monitor long term changes as production continues. Recently ERT and EM imaging have been used in bore holes and a high temperature EM system has been used to map fractures in a hot reservoir in Japan. Streaming potentials are routinely used to monitor leakage paths from reservoirs and dams. In a sense the field methodology is in place to monitor quantitatively the cold water injection process.

The more fundamental issue is to determine the nature of the physical changes that occur when cold water is injected into a fractured hot rock formation. This problem does not appear to have received very much attention and yet it lies at the core of any quantitative interpretation of geophysical monitoring of the injection process.

ERT forward modeling

Application of the finite-element method to a three-dimensional (3-D) resistivity problem is thoroughly discussed in Pridmore et al. (1981). For completeness, the method is briefly outlined here.

The partial differential equation governing the behavior of electric potential is described by the Poisson's equation

$$-\nabla \cdot \sigma \nabla \phi = \nabla \cdot \mathbf{J}_s , \qquad (1)$$

where σ is the conductivity (S/m), ϕ the potential (V), and $\mathbf{J}_s$ the impressed current source (A). The variational integral derived from the partial differential equation (1) is

$$\chi = \int [\sigma(\nabla\phi)^2 - 2\phi\nabla \cdot \mathbf{J}_s] dv \,. \quad (2)$$

The solution to equation (2) corresponds to the function ϕ, which makes the integral χ stationary.

In practice, the 3-D region is divided into a large number of bricks (or hexahedras) that can be assembled from five tetrahedral elements. The (unknown) potential is approximated in each element by a linear polynomial that is defined using the nodal values of ϕ. By substituting the linear polynomial into equation (2) and integrating over the volume of the element, we obtain the element integral that is dependent upon the nodal values of ϕ. The overall integral χ is the sum of these element integrals. The minimum of the integral χ can be found by setting the first derivative of χ with respect to the nodal values to zero. This leads to the finite-element matrix equation

$$\mathbf{Ku} = \mathbf{s}, \quad (3)$$

where **K** is a large, sparse, banded system matrix, **u** is a vector consisting of the unknown solutions of the nodal potentials at all nodes, and **s** represents the impressed source.

The incomplete Cholesky-conjugate gradient (ICCG) method is used to solve equation (3). The convergence of the iterative process can be accelerated by implementing in the source vector a pair of current sources (or the source and sink) rather than a current pole. However, iterative methods such as ICCG may require more computation time than direct methods when the solutions need to be obtained for a large number of source locations. In such cases a direct method would be preferable if the storage requirement can be met.

Numerical example

Figure 4 shows a cubic model containing a thin plate-like conductor. The conductor of 10 Ω-m is buried at the center of host medium of 100 Ω-m. Both source and receiving dipoles are set on the surface of the cube, as shown in Fig. 5. Results of resistivity modeling are shown in Figs. 6 through 11, in which unit is apparent resistivity (Ω-m):

$$\rho_a = \frac{100 I_{100}}{\Delta\phi_{100}} \frac{\Delta\phi}{I}, \quad (4)$$

where $\Delta\phi$ and $\Delta\phi_{100}$ are the potential differences, and I and I_{100} the impressed currents for the inhomogeneous and homogeneous (100 Ω-m) cubes, respectively. Here, the factor $(100 I_{100}/\Delta\phi_{100})$ can be regarded as a geometric factor.

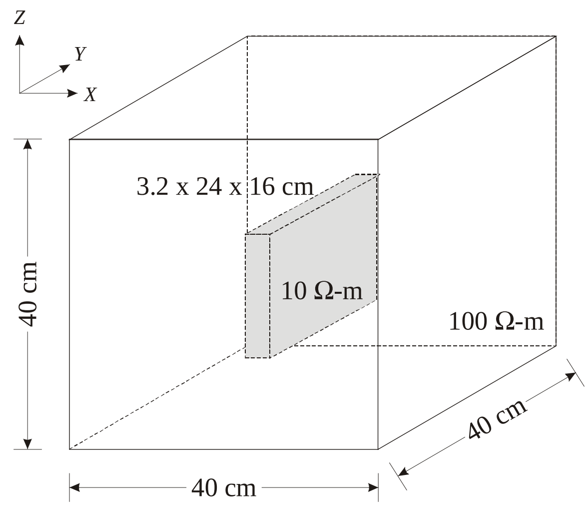

Figure 5 A simple model of a water injection zone in a field: a Plate-like conductor in a cube

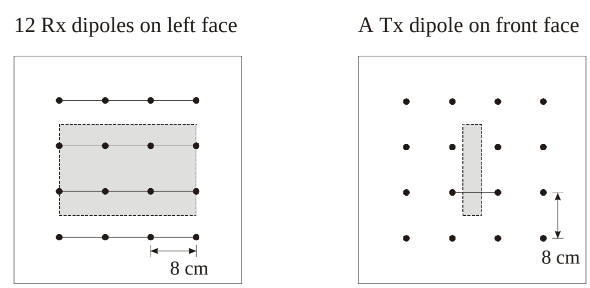

Figure 6 Locations of the 16 electrodes on the cubic specimen. Tx are transmitters and Rx are receivers.

<u>Least-squares inversion for injection imaging</u>

The dc resistivity inverse problem can be expressed as

$$\Delta\mathbf{d} = \mathbf{G}\Delta\mathbf{m}, \quad (5)$$

where $\Delta\mathbf{d}$ is the vector of differences between measured and modeled data, $\Delta\mathbf{m}$ the correction vector to the initial model $\mathbf{m}_0$, and **G** the Jacobian matrix (or the matrix of partial derivatives of the modeled response with respect to the model parameters). A common approach for the model parameterization is to divide a model into many blocks of unknown resistivity. To scale both parameters and data so that Jacobians will have a stable inverse, the logarithms of model resistivities and measured apparent resistivities are used.

As in most geophysical inverse problems, a roughness (the reciprocal of smoothness) term should be introduced to stabilize the inversion process (5) (Tikhonov and Arsenin, 1977). For the smoothest inversion, our objective function to be minimized is

$$U = \left\|\Delta\mathbf{d} - \mathbf{G}\Delta\mathbf{m}\right\|^2 + \lambda\left\|\mathbf{r}\right\|^2 , \qquad (6)$$

where ||•|| denotes the Euclidean norm and the second term on the right-hand side is the roughness weighted by the Lagrange multiplier λ. Here, the roughness is usually written as

$$\mathbf{r} = \mathbf{C}\Delta\mathbf{m}, \qquad (7)$$

where **C** is a second difference smoothing operator.

Minimization of equation (7) produces the system of linear equations

$$(\mathbf{G}^{\mathrm{T}}\mathbf{G} + \lambda\,\mathbf{C}^{\mathrm{T}}\mathbf{C})\Delta\mathbf{m} = \mathbf{G}^{\mathrm{T}}\Delta\mathbf{d}. \qquad (8)$$

This solution is equivalent to the least-squares solution of the system

$$\begin{vmatrix} \mathbf{G} \\ \sqrt{\lambda}\mathbf{C} \end{vmatrix} \Delta\mathbf{m} = \begin{vmatrix} \Delta\mathbf{d} \\ \mathbf{0} \end{vmatrix}. \qquad (9)$$

Equation (9) can be solved using singular-value decomposition or the modified Gram-Schmidt method. The solution obtained from equation (9) is known to be more accurate than the solution obtained via equation (8) (e.g., Lines and Treitel, 1984). The vector $\Delta\mathbf{m}$ is added to the initial vector $\mathbf{m}_0$ to obtain updated parameters. The procedure is repeated until a misfit between the measured and modeled data is reduced to an acceptable rms level. The rms misfit is given by

$$S = \sqrt{\frac{\Delta\mathbf{d}^{\mathrm{T}}\Delta\mathbf{d}}{N}} , \qquad (10)$$

where N is the number of data.

CONCLUSIONS

In this paper we have outlined large-scale physical modeling being undertaken to duplicate the in situ conditions of geothermal fields, such as The Geysers in Northern California. Field steam, superheat, 3-D confining stresses, and injection conditions can now be duplicated. Imaging of the injection process and associated rock damage will be imaged by quantitative microseismics and ERT. The forward and inverse ERT is described and the results from a numerical simulation is given.

REFERENCES

Lines, L. R., and Treitel, S. (1984), "Tutorial: A review of least-squares inversion and its application to geophysical problems," *Geophys. Prosp.*, **32**, 159-186.

Pridmore, D. F., Hohmann, G. W., Ward, S. H., and Sill, W. R. (1981), "An investigation of finite-element modeling for electrical and electromagnetic data in three dimensions," *Geophysics*, **46**, 1009-1024.

Stark, M.A. (1990), "Imaging Injected Water in The Geysers reservoir Using Microearthquake Data," *Trans. Geother. Resour. Counc*., **14**, 1697-1704.

Stump, B. W., and L. R. Johnson, (1969), "Higher-degree moment tensors - the importance of source finiteness and rupture propagation on seismograms"' *Geophysics Journal of the Royal Astronomical Society*, **69**, 721-743.

Tikhonov, A.N., and Arsenin, V.Y. (1977), *Solutions to Ill-Posed Problems*, John Wiley and Sons, Inc.

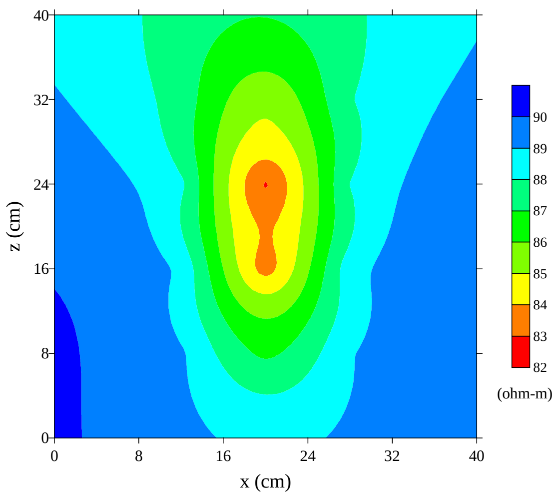

Figure 6 View of back face, Tx on front face

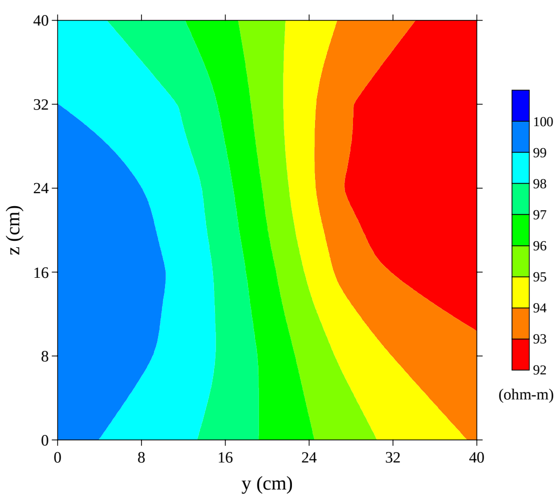

Figure 7 View of left face, Tx on front face

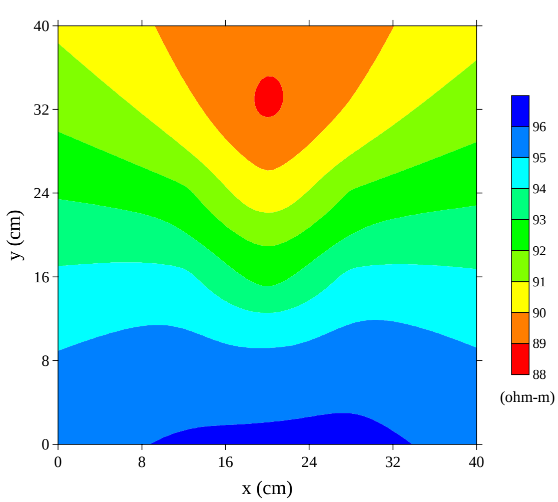

Figure 8 View of bottom face, Tx on front face

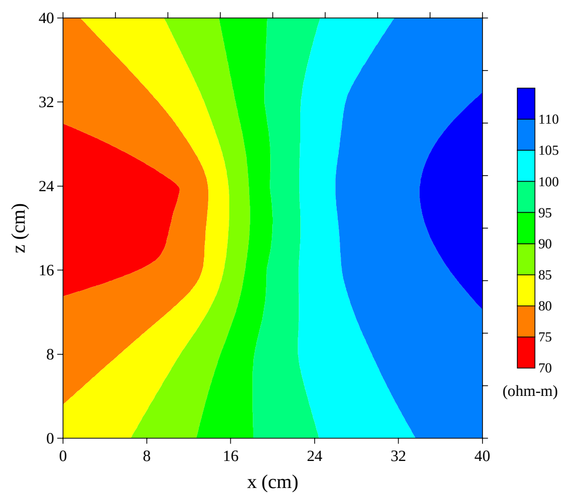

Figure 9 View of back face, Tx on right face

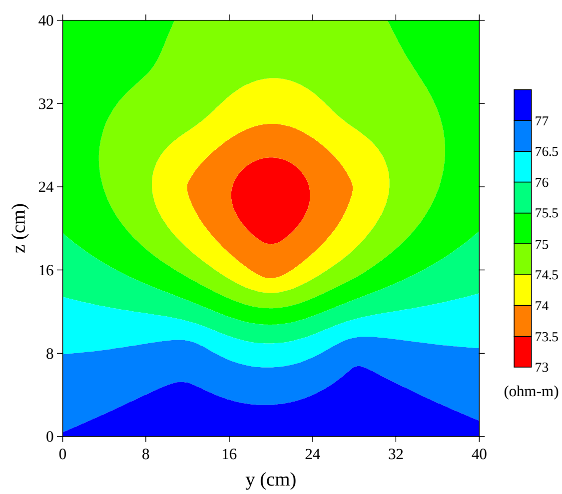

Figure 10 View of left face, Tx on right face

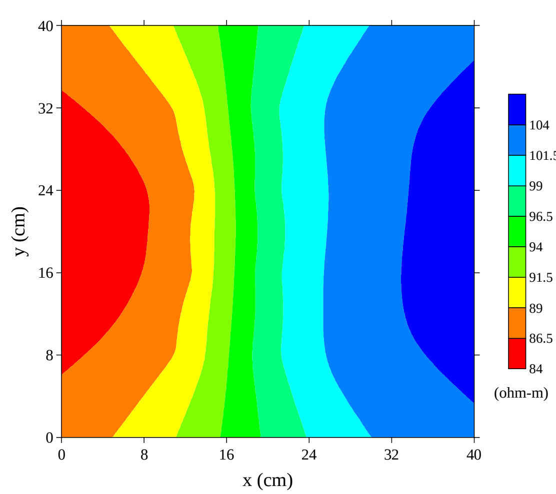

Figure 11 View of bottom face, Tx on right face